Cross sections for the formation of $^{69}Zn^{m,g}$ and $^{71}Zn^{m,g}$ in neutron induced reactions near their thresholds: Effect of reaction channel on the isomeric cross-section ratio

C. D. Nesaraja,* S. Sudár,† and S. M. Qaim‡
Institut für Nuklearchemie, Forschungszentrum Jülich GmbH, D-52425 Jülich, Germany
(Received 12 November 2002; published 25 August 2003)

Excitation functions were measured for the reactions $^{72}Ge(n,\alpha)^{69}Zn^{m,g}$, $^{69}Ga(n,p)^{69}Zn^{m,g}$, $^{70}Zn(n,2n)^{69}Zn^{m,g}$, $^{74}Ge(n,\alpha)^{71}Zn^{m,g}$, and $^{71}Ga(n,p)^{71}Zn^{m,g}$ over the neutron energy range of 6.3–12.4 MeV. Quasimonoenergetic neutrons in this energy range were produced via the $^{2}H(d,n)^{3}He$ reaction using a deuterium gas target at the Jülich variable energy compact cyclotron. Use was made of the activation technique in combination with high-resolution HPGe-detector γ-ray spectroscopy. In a few cases low-level β^- counting was also applied. In order to decrease the interfering activities in those cases, either radiochemical separations were performed or isotopically enriched targets were used. For most of the reactions, the present measurements provide the first consistent sets of data near their thresholds. From the available experimental data, isomeric cross-section ratios were determined for the isomeric pair $^{69}Zn^{m,g}$ in (n,α), (n,p), and $(n,2n)$ reactions, and for the pair $^{71}Zn^{m,g}$ in (n,α) and (n,p) reactions. Nuclear model calculations using the code STAPRE, which employs the Hauser-Feshbach (statistical model) and exciton model (precompound effects) formalisms, were undertaken to describe the formation of both isomeric and ground states of the products. The calculational results on the total (n,α), (n,p), and $(n,2n)$ cross sections agree fairly well with the experimental data. The experimental isomeric cross-section ratios, however, are reproduced only approximately by the calculation. For both the isomeric pairs investigated, the isomeric cross-section ratio in the (n,p) reaction is higher than in other reactions.

DOI: 10.1103/PhysRevC.68.024603 PACS number(s): 24.10.−i, 24.60.Dr, 25.10.+s, 25.40.−h

I. INTRODUCTION

Studies of excitation functions of neutron threshold reactions are of considerable importance for testing nuclear models as well as for practical applications. Furthermore, isomeric cross-section ratios are of fundamental interest. A literature survey (cf. Refs. [1,2]) showed that very little or incomplete experimental information is available for neutron induced reactions in the energy range between 5 and 12 MeV. We chose to study the (n,p) reactions on Ga and the (n,α) reactions on Ge, both Ga and Ge being important semiconducting materials. In addition, the $(n,2n)$ reaction on ^{70}Zn was also investigated. For all those reactions, some data exist in the literature [3–16] at energies above 12 MeV, mainly around 14 MeV, but not near the thresholds. The only exception is the $^{70}Zn(n,2n)^{69}Zn^{m}$ reaction, where Santry and Butler [17] reported data from about 9 MeV till 20 MeV. We recently described some experimental and theoretical investigations [18] on several reactions in this mass region. The present work is more related to the formation of the isomeric pairs $^{69}Zn^{m,g}$ and $^{71}Zn^{m,g}$, which have the same nuclear structure. They thus constitute an interesting model case for the study of isomeric cross-section ratios.

It is now known that the isomeric cross-section ratio is primarily governed by the spins of the levels involved, rather than their separation and excitation energies (cf. Ref. [19], and references cited therein). Furthermore, through detailed studies on the formation of $^{73}Se^{m,g}$ in six nuclear reactions [20], $^{58}Co^{m,g}$ in seven nuclear reactions [21], and $^{94}Tc^{m,g}$ in three nuclear processes [22], involving different combinations of target, projectile, and ejectile, the effects of moment of inertia, assumptions regarding angular momentum distribution in preequilibrium (PE) decay, spin and parity assignments of discrete levels, branching ratios of γ rays from discrete levels, and ratios of strengths of γ rays of different multipole types have been demonstrated. The effect of reaction channel on the isomeric cross-section ratio in neutron induced reactions was also investigated but found to be rather weak and inconclusive [23,24]. It seemed now interesting to us to study a model case of isomeric pairs with identical metastable and ground state spins. We chose to investigate the isomeric pairs $^{69}Zn^{m,g}$ and $^{71}Zn^{m,g}$. Figure 1 gives simplified schemes of the two isomeric pairs. Both of them have the ground state spin $(1/2^-)$ and the metastable state spin $(9/2^+)$. The aim of this work was to study the formation of the two isomeric states in various neutron induced reactions and thereby to observe the behavior of the isomeric cross-section ratio when the reaction channel changed.

II. EXPERIMENT

Cross sections were measured by activation and identification of the radioactive products. This technique is very suitable for investigating low-yield (n,p) and (n,a) reaction products and is almost ideal for studying closely spaced low-

*Present address: Department of Physics, Tennessee Technological University, Cookeville, TN 38505.
†Permanent address: Institute of Experimental Physics, University of Debrecen, H-4010 Debrecen, Hungary.
‡Corresponding author. Email address: s.m.qaim@fz-juelich.de

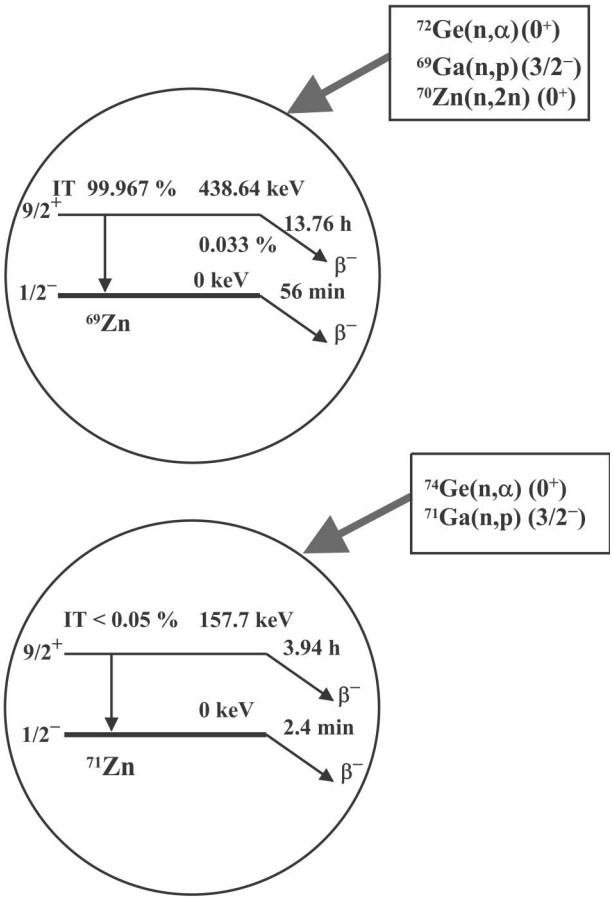

FIG. 1. Simplified level schemes of isomeric pairs $^{69}Zn^{m,g}$ and $^{71}Zn^{m,g}$. Formation of these isomeric pairs via different neutron induced reactions is given together with the spins and parities of the target nuclei in parentheses.

lying isomeric states, provided their lifetimes are not too short. The details have been described over the years in several publications (cf. Refs. [18,20,21]). Here, we give only some salient features relevant to the present measurements.

A. Samples and irradiations

About 4 g of Ge (>99.9% pure, Heraeus) or Ga_2O_3 (>99.9% pure, Aldrich/Heraeus) was pressed at 10 ton/cm^2 and a pellet (2.0 cm diameter, 0.3 cm thick) was obtained. Each pellet was placed in an aluminum capsule. Monitor foils (Al or Fe, each 100 μm thick) of the same size as the capsule were then attached in the front and at the back of each sample. For nondestructive β measurement on the $^{72}Ge(n,\alpha)^{69}Zn^{g}$ reaction, about 0.3 g of Ge was pressed to a pellet (1.3 cm diameter, 0.05 cm thick) which was then sandwiched between two thin cellulose tapes. For nondestructive β measurements on $^{74}Ge(n,\alpha)^{71}Zn^{g}$ and $^{71}Ga(n,p)^{71}Zn^{g}$ reactions, as well as β and γ measurements on the $^{70}Zn(n,2n)^{69}Zn^{m,g}$ processes, isotopically enriched samples were used. Their compositions are given in Table I. In each case about 0.030 g of the material distributed over a circle of 1.3 cm diameter was simply sealed in very thin polyethylene foils. Those samples were sufficiently thin to ignore the self-absorption corrections in β measurements. Al or Fe monitor foils (each 100 μm thick) of the same size as the sample were attached in the front and at the back of the sample, similar to that in the case of the Al capsule (see above).

TABLE I. Isotopic composition of the enriched material used.

Target material	Element of interest	Isotopic composition (%)	Supplier
GeO_2	Ge	^{70}Ge(0.21), ^{72}Ge(0.34), ^{73}Ge(0.95), ^{74}Ge(98.44), ^{76}Ge(0.06)	Chemotrade
Ga_2O_3	Ga	^{69}Ga(0.46), ^{71}Ga(99.54)	Oak Ridge
ZnO	Zn	^{64}Zn(5.83), ^{66}Zn(3.78), ^{67}Zn(0.71), ^{68}Zn(4.65), ^{70}Zn(85.03)	Chemotrade

Irradiations were performed at the Jülich variable energy compact cyclotron CV28. The quasimonoenergetic neutrons were produced via the $^2H(d,n)^3He$ reaction (Q = 3.27 MeV) on a D_2 gas target (3.7 cm long, 1.8×10^5 Pa pressure). The characteristics of this neutron source have been described earlier [25,26]. The samples were placed in the 0° direction relative to the incident deuteron beam, at a distance of 0.5 or 1 cm from the beam stop. By changing the deuteron energy between 3.5 and 10.0 MeV, it was possible to obtain neutrons of energies between 6 and 12 MeV. The beam current was kept constant at 4 μA. The duration of irradiation varied between 5 min and 3 h, depending on the half-life of the product. At each energy two irradiations were done, one with the target filled with the D_2 gas and the other as empty (gas in/gas out). This allowed a correction for the activity formed from the background neutrons.

B. Neutron energies and flux densities

The average neutron energy effective at each sample was calculated using a Monte Carlo program (cf. Ref. [27]) which takes into account the energy loss and angular straggling of the deuterons in the entrance window of the gas target, the energy loss in the D_2 gas, the angular distribution of the $^2H(d,n)^3He$ reaction, the production of the neutrons in the space of the gas cell, and the breakup of the deuterons on the D_2 gas according to the results of Cabral *et al.* [28]. The activation geometry parameters (length and diameter of the sample, pressure of D_2 gas, and distance between the sample and beam stop) were also considered.

The Monte Carlo program (DD-NEUT) was also used to calculate the whole neutron spectrum which is divided in a breakup part and a monoenergetic part. The ratio of the activity induced by the monoenergetic neutrons to that by the breakup neutrons was calculated and used for the correction of the contribution of the breakup neutrons. The contribution of these low-energy neutrons for each investigated reaction including the monitor reaction $^{27}Al(n,p)^{27}Mg$ with reaction threshold below the monoenergetic neutron peak was calculated. The correction was of the order of a few percent, depending on the reaction threshold and the excitation function of the investigated reaction.

TABLE II. Decay data of measured reaction products.

Reaction product[a]	Half-life	Mode of decay (%)	$E_{\beta max}$ (keV)	E_γ (keV)	I_γ (%)
$^{69}Zn^m$	13.76 h	IT(99.97)		438.6	94.8
		β^-(0.03)	439		
$^{69}Zn^g$	56 min	β^-(100)	905		
$^{71}Zn^m$	3.94 h	β^-(100)	541	386.4	93.0
$^{71}Zn^g$	2.4 min	β^-(100)	2295	910.3	7.8

[a]Taken from Refs. [30,31].

For ascertaining the constancy of the neutron flux, a constant check of the D_2 gas pressure in the cell and the deuteron beam current on the target was performed. The neutron flux density effective during each irradiation was determined via a monitor reaction. For neutron energy up to 8 MeV, the monitor reaction used was $^{56}Fe(n,p)^{56}Mn$ ($T_{1/2}=2.58$ h, $E_\gamma=847$ keV, $I_\gamma=98.9\%$), and for energies above 8 MeV, the reaction $^{27}Al(n,\alpha)^{24}Na$ ($T_{1/2}=14.97$ h; $E_\gamma=1369$ keV; $I_\gamma=100\%$). In short irradiations of about 5 min duration, the neutron flux density was measured via the reaction $^{27}Al(n,p)^{27}Mg$ ($T_{1/2}=9.46$ min, $E_\gamma=844$ keV, $I_\gamma=73\%$). The cross sections of the monitor reactions were taken from the IRDF computer file (cf. Ref. [29]). The flux densities were calculated after correction of monitor product activities from background neutrons. The average flux density effective on each sample was then obtained by taking the mean value of the calculated flux density for the front and back foils.

C. Measurement of radioactivity

The activation products were identified by β^- or γ counting and checking their half-lives. Table II gives the decay data of the products [30,31] used in quantitative assay of the activity.

For investigations on the $^{69}Ga(n,p)^{69}Zn^g$ and $^{69}Ga(n,p)^{69}Zn^m$ reactions, radiochemical separations were performed, similar to those in the case of the $^{71}Ga(n,p)^{71}Zn^m$ reaction, described earlier [18].

1. γ-ray spectrometry

A HPGe detector was used to measure the activities of ^{24}Na, ^{56}Mn, and ^{27}Mg from the irradiated monitor foils, and the activities of $^{69}Zn^m$ and $^{71}Zn^m$ from the irradiated samples. The samples and foils were placed either directly on the end cap of the detector or at a distance of 3 cm. Peak area analysis was done using the software GAMMAVISION, version 2.00. The detector efficiency was determined experimentally using a selected set of γ-ray standard sources (obtained from Amersham International or PTB, Braunschweig). Corrections were applied for the extended form of samples (cf. Ref. [18]).

2. β counting

For pure β^-particle emitters, thin sources were used to reduce the self-absorption effect. In the case of the $^{69}Ga(n,p)^{69}Zn^g$ reaction, this was achieved via a radiochemical separation, whereas in investigations on the $^{70}Zn(n,2n)^{69}Zn^g$, $^{71}Ga(n,p)^{71}Zn^g$, and $^{74}Ge(n,\alpha)^{71}Zn^g$ processes, thin samples of highly enriched materials were employed. Only in the case of the $^{72}Ge(n,\alpha)^{69}Zn^g$ reaction a somewhat thicker sample was used but appropriate β attenuation within the sample was estimated. A 2π geometry gas flow proportional counter, having a thin window and equipped with an anticoincidence system, was applied. Counting was started either immediately after the end of bombardment (EOB) or after separation, and was continued for about 20 h to be able to analyze the decay curve. The various components were then obtained by a multidecay analysis based on an interactive fitting procedure. The major emphasis was on the analysis of $^{69}Zn^g$($T_{1/2}=56.0$ min) and $^{71}Zn^g$($T_{1/2}=2.4$ min). The detector efficiency was determined experimentally using a set of β^-ray standard sources (obtained from Amersham International).

D. Calculation of cross sections and their uncertainties

The count rates at the EOB after correction for contributions from background neutrons, were converted to decay rates by introducing corrections for emission probabilities of β^- and γ rays, detector efficiency, self-absorption, coincidence loss, and chemical yield (for reactions involving a chemical separation). Cross sections were then calculated using the well-known activation equation. The principal sources of uncertainty and their magnitudes involved in both the γ and β measurements have been described in detail earlier [18]. The individual uncertainties were combined in quadrature to obtain an overall uncertainty of 9%–28%. The maximum uncertainty of 28% occurred for reactions involving radiochemical separations and β counting with poor statistics.

E. Calculation of isomeric cross-section ratios

The calculation of the isomeric cross-section ratio $\sigma_m/(\sigma_m+\sigma_g)$ for the isomeric pair $^{71}Zn^{m,g}$ was straightforward since both the states decay independently (cf. Fig. 1) and their formation cross sections were determined independently. In the case of the pair $^{69}Zn^{m,g}$, the σ_m was determined independently but for σ_g some correction for the decay of the metastable state $^{69}Zn^m$($T_{1/2}=13.76$ h) to the ground state $^{69}Zn^g$($T_{1/2}=56$ min) was necessary.

The uncertainties in the isomeric cross-section ratios were obtained by combining in quadrature the uncertainties in the individual cross sections involved. The isomeric cross-section ratio is independent of the neutron flux. Therefore, using the final uncertainties of the cross sections, the uncertainty of the isomeric ratio is overestimated. In general, the total uncertainty for each ratio was about 30%.

III. NUCLEAR MODEL CALCULATIONS

Cross sections were calculated using the statistical model taking into account the preequilibrium effects. The calculational code STAPRE [32] was applied. Calculations of total (n,α), (n,p), and $(n,2n)$ cross sections on several target

TABLE III. Activation cross sections determined via γ-ray spectrometry.

$\langle E_n \rangle$[a] (MeV)	Cross section (mb) ^{72}Ge$(n,\alpha)^{69}$Zn^m	^{69}Ga$(n,p)^{69}$Zn^m [b]	^{70}Zn$(n,2n)^{69}$Zn^m [c]	^{74}Ge$(n,\alpha)^{71}$Zn^m
6.32±0.41		4.8±0.8		
7.33±0.48		6.3±0.9		
7.46±0.26	0.62±0.06			0.03±0.01
8.01±0.53		9.4±1.3		
8.28±0.27	0.83±0.09			0.08±0.02
9.09±0.62		12.7±1.8		
9.16±0.55	1.35±0.14			0.21±0.04
9.96±0.34	2.3±0.3			0.48±0.09
10.13±0.74		17.8±3.5		
10.32±0.54			93±11	
10.71±0.35	2.5±0.3			0.63±0.12
11.24±0.84		26.4±5.2		
11.37±0.38	2.8±0.4			0.81±0.13
11.42±0.61			286±30	
11.80±0.31	3.2±0.4			0.91±0.09
11.96±0.70	4.5±0.5			1.35±0.27
11.98±0.51			581±73	
12.06±0.93		29.0±6.2		
12.29±0.67			732±84	

[a]The deviations do not describe errors in the energy scale; they show energy spreads due to angle of emission.
[b]The product was radiochemically separated.
[c]An enriched ^{70}Zn sample was used.

nuclei in this mass region, including ^{74}Ge and ^{71}Ga, have already been described [18,21]. The same procedure was now applied to the target nuclei ^{72}Ge, ^{69}Ga, and ^{70}Zn.

The transmission coefficients for neutrons, protons, and α particles were provided as input data to the STAPRE code by means of the spherical optical code SCAT-2 [33]. They were generated in SCAT-2 using parameters chosen from a global parameter set. For neutron, the optical model parameter set of Ref. [34] and for proton that of Perey [35] were used. In the case of α particles, a modified set of optical model parameters of Ref. [36] was used. The potentials used were checked by comparing their predictions of nonelastic and total cross sections with experimental data [2], wherever available.

In the present work, the emphasis was on the isomeric cross sections. Since such calculations are strongly dependent on the input level scheme of the product nucleus [20,21], we chose those parameters carefully. The energies, spins, parities, and branching ratios of discrete levels were selected from Refs. [37,38]. Reference was also made to Ref. [31] from where levels up to energies of 4 MeV were taken when the level information was complete. In case where spin and parity were not known, estimates from adjacent levels were made. In the continuum region, the level density was calculated by the back-shifted formula and the level density parameter given in Ref. [39]. Another important consideration in calculating the isomeric cross sections is the spin distribution of the level density (cf. Refs. [20,24,40]). This was characterized by the ratio of the effective moment of inertia Θ_{eff} to the rigid-body moment of inertia Θ_{rig}($\eta = \Theta_{eff}/\Theta_{rig}$) and the calculations were performed for $\eta = 1.0$. The transmission coefficients of photons are also of considerable significance in calculations on isomeric cross sections. They were derived from the γ-ray strength functions. For the $E1$ transition the Brink-Axel model with global parameters was applied, while for the $M1$, $E2$, $M2$, $E3$, and $M3$ radiation the Weisskopf model was used.

IV. RESULTS AND DISCUSSION

A. Cross sections and excitation functions

The reaction cross sections determined through identification of the activation products via γ-ray spectrometry and β^- counting are given in Tables III and IV, respectively.

The measurements via γ-ray spectrometry were generally done using target elements of natural isotopic composition. Due to the use of high-resolution detectors no difficulty was observed. In the case of the ^{70}Zn$(n,2n)^{69}$Zn^m reaction, however, due to the very low abundance of the target isotope (0.6%), an isotopically enriched target sample had to be used. As regards β^- counting, the results are generally associated with higher uncertainties. We attempted to reduce the uncertainties either through the use of highly enriched target isotopes (e.g., ^{70}Zn, ^{71}Ga, and ^{74}Ge) or through a radiochemical separation such as in the case of the ^{69}Ga$(n,p)^{69}$Zn^g and ^{72}Ge$(n,\alpha)^{69}$Zn^g reactions. Over the energy region of 6–12.5 MeV studied in this work, previously only some data for the ^{70}Zn$(n,2n)^{69}$Zn^g reaction existed [17]. All of the other eight reactions have been investigated for the first time.

TABLE IV. Activation cross sections determined via β^- counting.

$\langle E_n \rangle$[a] (MeV)	Cross section (mb) $^{72}Ge(n,\alpha)^{69}Zn^g$	$^{69}Ga(n,p)^{69}Zn^g$ [b]	$^{70}Zn(n,2n)^{69}Zn^g$ [c]	$^{74}Ge(n,\alpha)^{71}Zn^g$ [d]	$^{71}Ga(n,p)^{71}Zn^g$ [e]
6.32±0.41		3.0±0.6			
7.33±0.48		2.9±0.5			
7.38±0.21	3.1±0.9				
8.01±0.53		3.8±0.6			
8.38±0.22	3.6±1.1				
8.39±0.44				0.45±0.08	1.6±0.6
9.09±0.62		5.0±1.33			
9.44±0.49				1.04±0.21	5.0±0.8
10.05±0.67	4.0±1.0				
10.13±0.74		6.8±1.6			
10.32±0.54			96±29		
10.45±0.55				1.35±0.40	8.5±1.5
10.96±0.75	4.5±1.1				
11.24±0.84		8.2±1.6			
11.42±0.61			188±53		
11.48±0.64				3.3±1.3	11.7±3.2
11.87±0.37	7.2±2.4				
11.98±0.51			301±80		
12.06±0.93		8.7±1.7			
12.29±0.67			425±117		
12.44±0.68				4.4±1.5	13.0±3.3

[a]The deviations do not describe errors in the energy scale; they show energy spreads due to angle of emission.
[b]The product was radiochemically separated.
[c]An enriched ^{70}Zn sample was used.
[d]An enriched ^{74}Ge sample was used.
[e]An enriched ^{71}Ga sample was used.

The excitation functions for the formation of $^{69}Zn^m$ and $^{69}Zn^g$ in (n,α), (n,p), and $(n,2n)$ reactions are given in Figs. 2–7. Similarly, the excitation functions for the formation of $^{71}Zn^m$ and $^{71}Zn^g$ in (n,α) and (n,p) reactions are given in Figs. 8–11. In addition to our own experimental data, the available literature data, mainly around 14 MeV [3–16], are also shown. The results of nuclear model calculations performed in the present work are also reproduced in Figs. 2–11 for comparison. We discuss below each reaction individually in some detail.

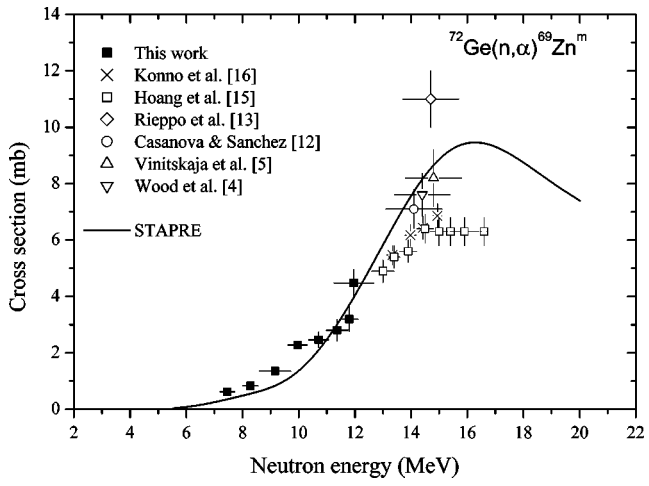

FIG. 2. Excitation function of the $^{72}Ge(n,\alpha)^{69}Zn^m$ reaction. In addition to the present data, those from the literature [4,5,12,13,15,16] are also given. The result of the STAPRE calculation is shown as a solid line.

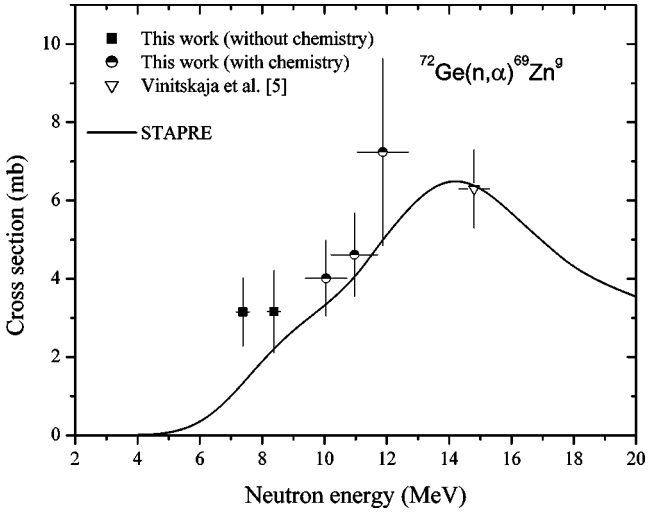

FIG. 3. Excitation function of the $^{72}Ge(n,\alpha)^{69}Zn^g$ reaction based on the present and literature [5] data. The result of the STAPRE calculation is shown as a solid line.

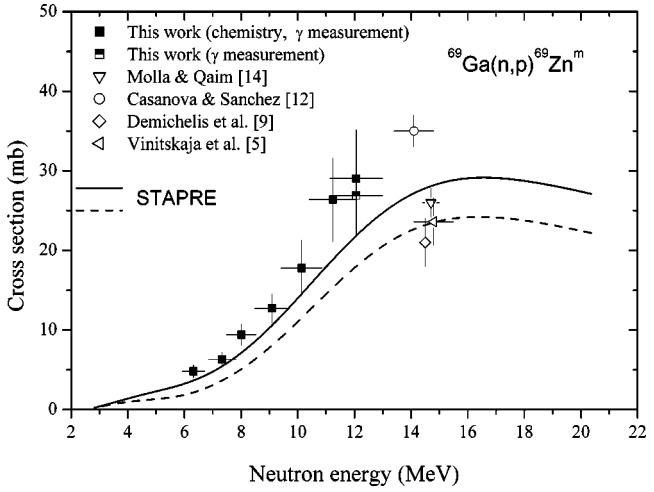

FIG. 4. Excitation function of the ^{69}Ga$(n,p)^{69}$Zn^m reaction based on the present and literature [5,9,12,14] data. The STAPRE calculation was done using two different spin values of the excited state of ^{69}Zn at 967 keV (solid curve with $I=7/2$, dashed curve with $I=3/2$).

In the case of the ^{72}Ge$(n,\alpha)^{69}$Zn^m reaction (Fig. 2), the transition from the present low-energy data to the literature higher-energy data is relatively smooth, except for the cross-section value at 14.7 MeV given by Ref. [13] and for the constant cross section over the energy range of 14.5–16.5 MeV reported by authors of Ref. [15]. In the case of the ^{72}Ge$(n,\alpha)^{69}$Zn^g reaction (Fig. 3), we measured the cross section both with and without a chemical separation. The consistency in results gives added confidence to the techniques used. The 15-MeV data point [5] is also consistent. Regarding the nuclear model calculations, in Figs. 2 and 3 the results of STAPRE are given as continuous lines. For the reactions under consideration, the agreement between experiment and theory is relatively good.

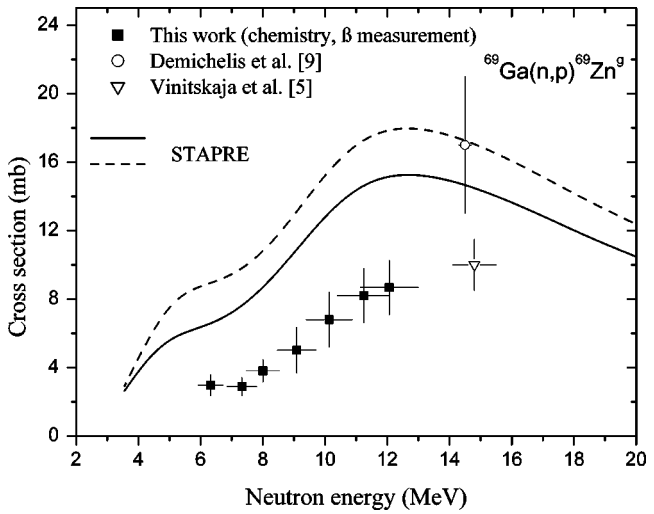

FIG. 5. Excitation function of the ^{69}Ga$(n,p)^{69}$Zn^g reaction based on the present and literature [5,9] data. The two curves giving results of the STAPRE calculation have the same meaning as in Fig. 4.

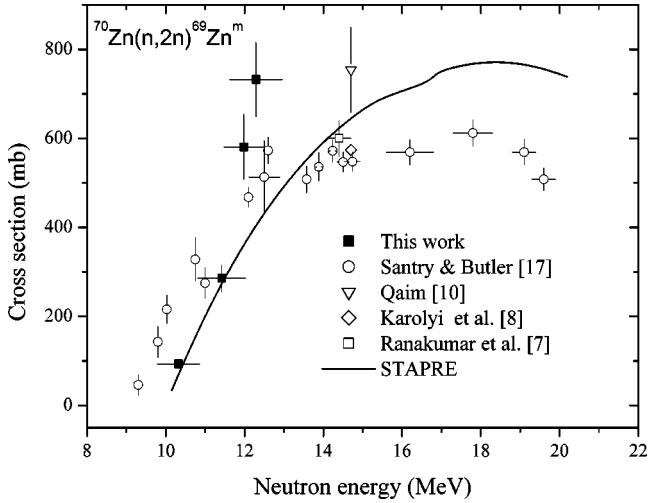

FIG. 6. Excitation function of the ^{70}Zn$(n,2n)^{69}$Zn^m reaction based on the present and literature [7,8,10,17] data. The result of the STAPRE calculation is shown as a solid line.

The data for the ^{69}Ga$(n,p)^{69}$Zn^m reaction (Fig. 4) are also consistent, though the value of Ref. [12] at 14 MeV is somewhat high. In the case of the ^{69}Ga$(n,p)^{69}$Zn^g reaction (Fig. 5), on the other hand, there appears to be considerable discrepancy. Around 14 MeV two widely differing values have been reported [5,9]

The theoretical curve fits well to the data points in the case of the ^{69}Ga$(n,p)^{69}$Zn^m reaction, when the spin value of the 967-keV level is adopted as 7/2 (Fig. 4). The calculational results for the ^{69}Ga$(n,p)^{69}$Zn^g reaction, however, are too high as compared to the experimental data (Fig. 5).

The cross section data for the ^{70}Zn$(n,2n)^{69}$Zn^m reaction are shown in Fig. 6. The literature data [7,8,10,17] show considerable scatter; especially the values given by Ref. [17] at energies above 13 MeV appear to be rather low. The cross section database for the ^{70}Zn$(n,2n)^{69}$Zn^g reaction is weak, our data being the first measurement on this reaction (Fig. 7). The nuclear model calculation reproduces the excitation function for the formation of the ground state (Fig. 7) very

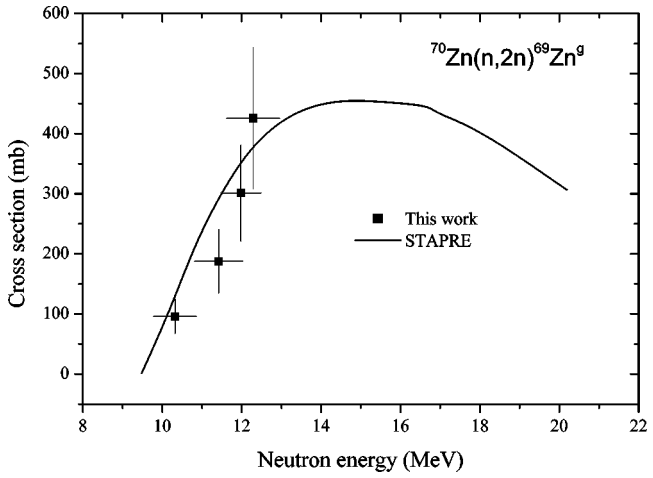

FIG. 7. Excitation function of the ^{70}Zn$(n,2n)^{69}$Zn^g reaction based on the present experimental data and STAPRE calculation.

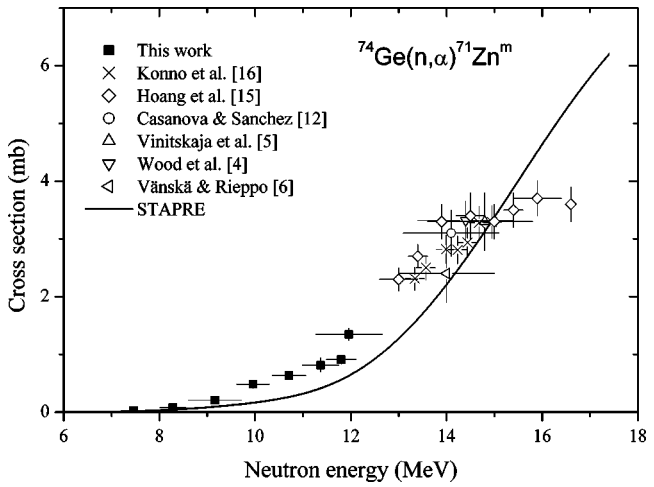

FIG. 8. Excitation function of the $^{74}Ge(n,\alpha)^{71}Zn^{m}$ reaction based on the present and literature [4–6,12,15,16] data. The result of the STAPRE calculation is shown as a solid line.

well but not of the isomeric state (Fig. 6).

Regarding the $^{74}Ge(n,\alpha)^{71}Zn^{m}$ reaction, the transition from our low-energy data to the higher-energy literature data [4–6,12,15,16] is good (Fig. 8), except for the values of Ref. [15] which above 14 MeV are somewhat flat. The model calculation reproduces the excitation function fairly well.

In the case of the $^{74}Ge(n,\alpha)^{71}Zn^{g}$ reaction, on the other hand, the 14-MeV literature data [3,5,12] are very discrepant, so that it is not possible to define the exact shape of the experimental excitation function (Fig. 9). The nuclear model calculation agrees with our low-energy data.

The experimental data for the $^{71}Ga(n,p)^{71}Zn^{m}$ reaction have been reported by us earlier [18]. Those data together with the literature data in the higher-energy region [5,9,11,12,14] are reproduced in Fig. 10. The data around 14 MeV show considerable scatter. The available cross-section data for the $^{71}Ga(n,p)^{71}Zn^{g}$ reaction [5,9,12,14] are shown in Fig. 11. Worth emphasizing is that, in contrast to the earlier studies, present measurements have been done using a highly enriched sample. In view of the detection of the product only via β^{-} counting, we considered the use of an isotopically enriched sample as absolutely mandatory. Our data are rather high compared to the 14-MeV literature data [5,9,12,14]. As far as nuclear model calculations are concerned, the results obtained using two different numbers of discrete levels in the product nucleus are shown (Figs. 10 and 11). The influence of the input level structure is obvious. For the two reactions, the agreement between theory and our experimental data is good.

The data shown in Figs. 2–11 and the discussion given above lead us to conclude that, in general, our measurements agree with the nuclear model calculations. Only in the case of the $^{69}Ga(n,p)^{69}Zn^{g}$ reaction, the result of the model calculation is about twice the experimental value. Considering

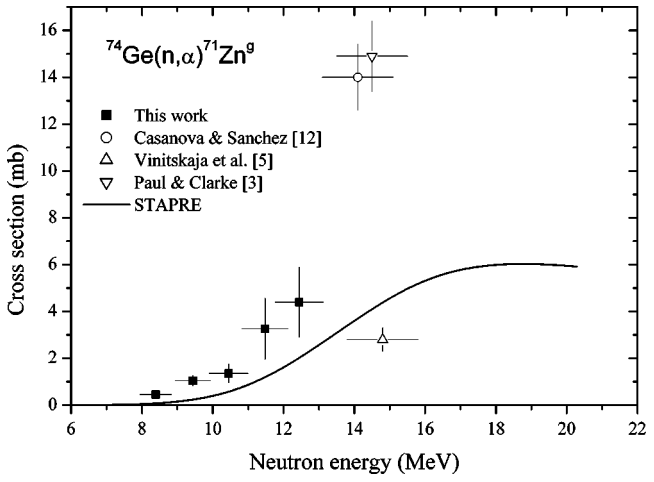

FIG. 9. Excitation function of the $^{74}Ge(n,\alpha)^{71}Zn^{g}$ reaction based on the present and literature [3,5,12] data. The result of the STAPRE calculation is shown as a solid line.

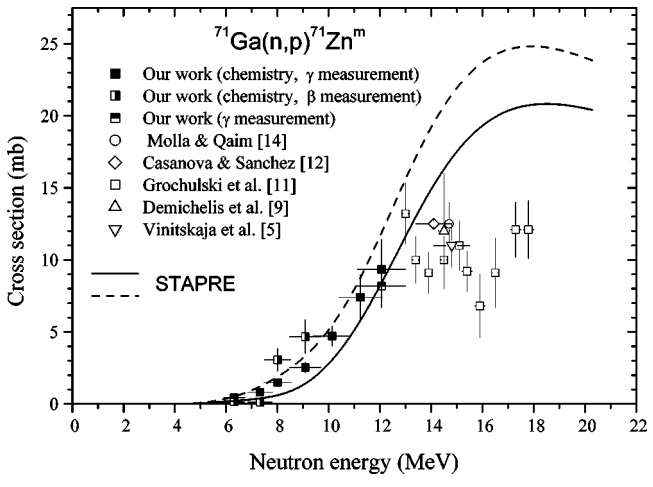

FIG. 10. Excitation function of the $^{71}Ga(n,p)^{71}Zn^{m}$ reaction based on our measurement [18] and literature [5,9,11,12,14] data. The STAPRE calculation was done using two different numbers of discrete levels in the product nucleus ^{71}Zn (solid curve using 18 levels, dashed curve using 39 discrete levels).

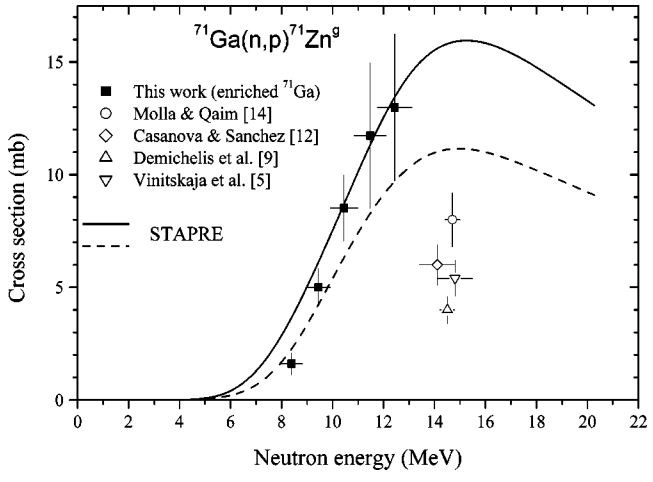

FIG. 11. Excitation function of the $^{71}Ga(n,p)^{71}Zn^{g}$ reaction based on the present and literature [5,9,11,12,14] data. The two curves giving results of the STAPRE calculation have the same meaning as in Fig. 10.

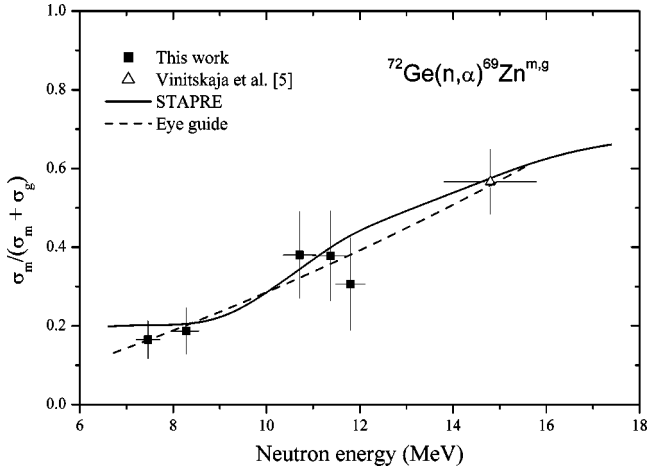

FIG. 12. Isomeric cross-section ratio for the pair $^{69}Zn^{m,g}$ in the $^{72}Ge(n,\alpha)$ reaction as a function of the neutron energy based on the present and literature [5] data. The metastable state has the spin $(9/2^+)$ and the ground state $(1/2^-)$. An eye guide through the experimental data and the result of the STAPRE calculation are given.

the relatively low summed cross section of all the (*n*, *charged particle*) reactions in this mass region (<30 mb which amounts to $<5\%$ of the total inelastic cross section), the agreement between experiment and theory may be regarded as good. The same is, however, not true for the 14-MeV data reported in the literature. Whereas some of them are quite consistent, many others are discrepant. The conclusion about agreement between theory and experiment is therefore rather vague in that energy region.

B. Isomeric cross-section ratios

The experimental results on the isomeric cross-section ratios $\sigma_m/(\sigma_m+\sigma_g)$ for the isomeric pair $^{69}Zn^{m,g}$ in (n,α), (n,p), and $(n,2n)$ reactions are given in Figs. 12–14, and for the isomeric pair $^{71}Zn^{m,g}$ in (n,α) and (n,p) reactions in Figs. 15 and 16, respectively. Around 14 MeV,

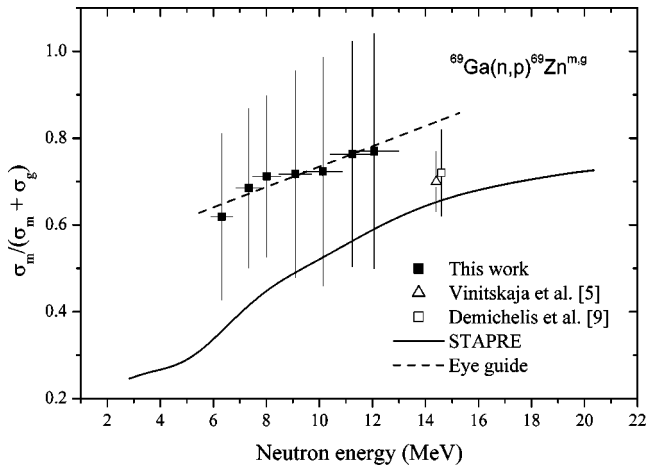

FIG. 13. Isomeric cross-section ratio for the pair $^{69}Zn^{m,g}$ in the $^{69}Ga(n,p)$ reaction as a function of the neutron energy based on the present and literature [5,9] data. Other details are the same as for Fig. 12.

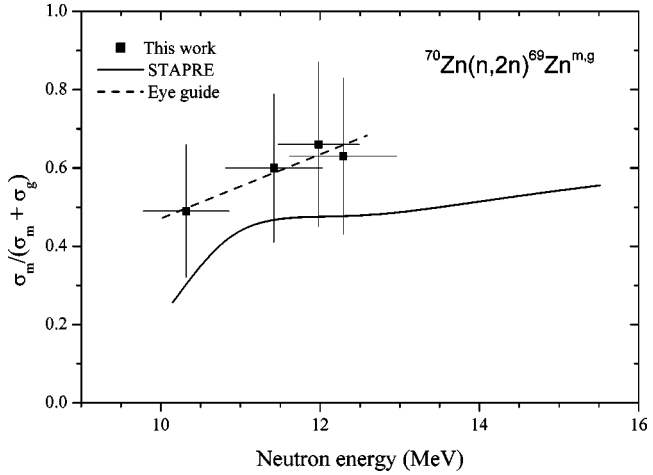

FIG. 14. Isomeric cross-section ratio for the pair $^{69}Zn^{m,g}$ in the $^{70}Zn(n,2n)$ reaction as a function of the neutron energy based on our low-energy data. Other details are the same as for Fig. 12.

results of only those literature reports are shown where cross sections of both the metastable and the ground state were measured. The results of the nuclear model calculations performed in the present work are also given.

The experimental isomeric cross-section ratio for the isomeric pair $^{69}Zn^{m,g}$ in the (n,α) reaction (Fig. 12) is low at low energies but increases rapidly with the increasing neutron energy. A somewhat similar trend is observed in the case of the (n,p) reaction (Fig. 13), although the increase is less marked. In the case of the $(n,2n)$ reaction, the increase in the isomeric cross-section ratio with the energy is very small (Fig. 14); a definite conclusion, however, is difficult since no 14-MeV data exist. The model calculations appear to reproduce the shapes of the experimental curves reasonably well, but the magnitudes only within the extreme limits of the reported errors.

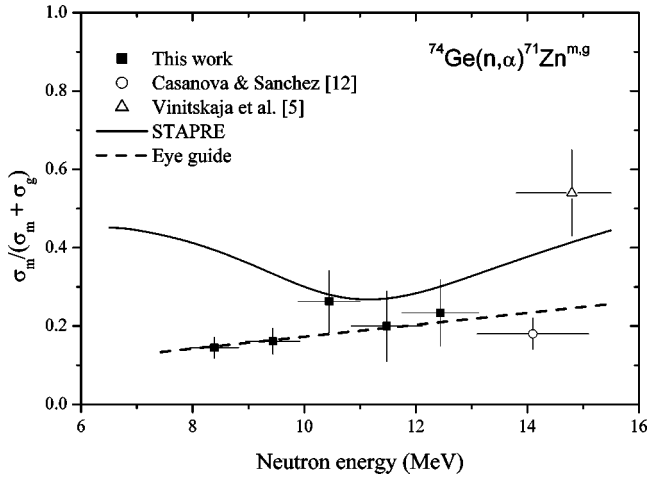

FIG. 15. Isomeric cross-section ratio for the pair $^{71}Zn^{m,g}$ in the $^{74}Ge(n,\alpha)$ reaction as a function of the neutron energy based on the present and literature [5,12] data. The metastable state has the spin $(9/2^+)$ and the ground state $(1/2^-)$. An eye guide through the experimental data and the result of the STAPRE calculation are given.

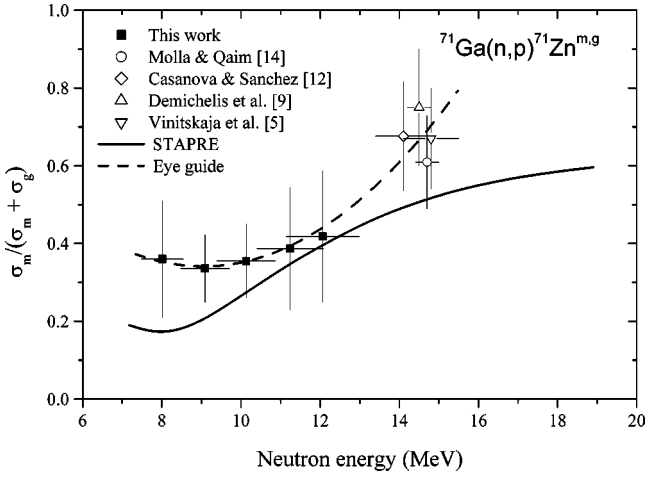

FIG. 16. Isomeric cross-section ratio for the pair $^{71}Zn^{m,g}$ in the $^{71}Ga(n,p)$ reaction as a function of the neutron energy based on the present and literature [5,9,12,14] data. Other details are the same as for Fig. 15.

The experimental isomeric cross-section ratio for the isomeric pair $^{71}Zn^{m,g}$ in the (n,α) reaction is given in Fig. 15. The ratio is low at low energies and increases only slowly with the increasing neutron energy. The trend is different in the (n,p) reaction (Fig. 16). The ratio increases rapidly with the increasing neutron energy. The results of the model calculations (Figs. 15 and 16) generally agree with the experimental data; only in the low-energy region, considerable deviation is observed, especially in the case of the (n,α) reaction.

The experimental data on the isomeric cross-section ratios given in Figs. 12–16 support the previous conclusion (cf. Ref. [19]) that the ratio is strongly dependent on the spins of the states involved. At low energies, the low-spin isomer $(1/2^-)$ is favored, but with the increasing incident neutron energy the population of the high-spin isomer $(9/2^+)$ increases. As far as theoretical predictions are concerned, the model calculations taking into account all the related parameters appear to reproduce the experimental data, though often within the extreme limits of uncertainties.

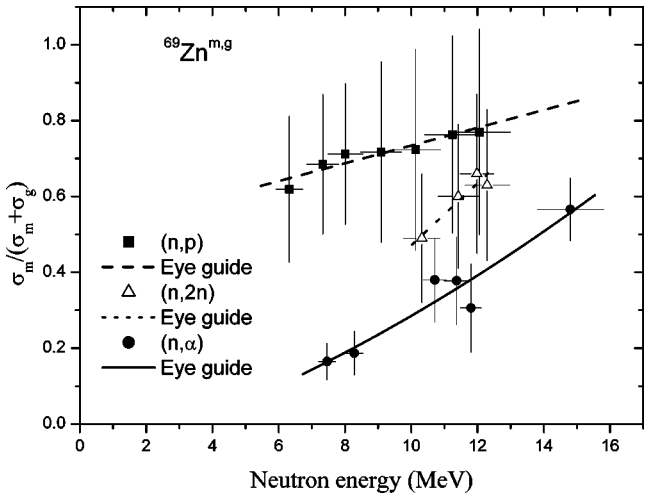

FIG. 17. Comparison of experimental isomeric cross-section ratios for the formation of $^{69}Zn^{m,g}$ in (n,α), (n,p), and $(n,2n)$ reactions. The data are shown as a function of the incident neutron energy. The curves are eye guides through the data points.

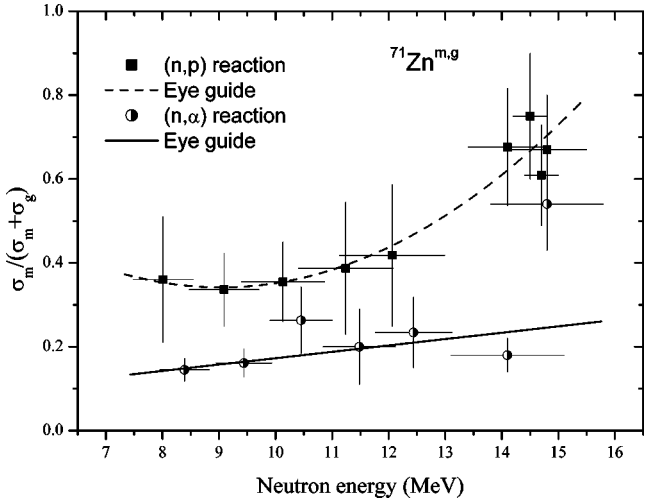

FIG. 18. Comparison of experimental isomeric cross-section ratios for the formation of $^{71}Zn^{m,g}$ in (n,α) and (n,p) reactions. The data are shown as a function of the incident neutron energy. The curves are eye guides through the data points.

C. Effect of reaction channel

The measured isomeric cross-section ratios and the eye-guided curves through them for the isomeric pair $^{69}Zn^{m,g}$ in the (n,α), (n,p), and $(n,2n)$ reactions, depicted in Figs. 12, 13, and 14, respectively, are collectively shown in Fig. 17 as a function of the incident neutron energy. Similar data for the isomeric pair $^{71}Zn^{m,g}$ in the (n,α) and (n,p) reactions, shown in Figs. 15 and 16, are reproduced in Fig. 18. A comparative consideration of the two isomeric pairs, viz, $^{69}Zn^{m,g}$ and $^{71}Zn^{m,g}$, with the two lowest low-lying levels of identical spin and parity, and with the respective targets of the same spin and parity (cf. Fig. 1), reveals that for a particular type of reaction the trend in the isomeric cross-section ratio as a function of projectile energy may or may not be similar. In the case of the pair $^{69}Zn^{m,g}$ the change in the isomeric cross-section ratio with energy is more pronounced in the (n,α) reaction; for the pair $^{71}Zn^{m,g}$, however, the same is true in the case of the (n,p) reaction. For both the pairs, the isomeric cross-section ratios are higher in the (n,p) reaction than in the (n,α) reaction.

V. CONCLUSION

Experimental and theoretical studies on the isomeric pair $^{69}Zn^{m,g}$ in three nuclear reactions, namely, $^{72}Ge(n,\alpha)$, $^{69}Ga(n,p)$, and $^{70}Zn(n,2n)$, and on the pair $^{71}Zn^{m,g}$ in two nuclear reactions, namely, $^{74}Ge(n,\alpha)$ and $^{71}Ga(n,p)$, showed that the total reaction cross section of a particular channel under consideration is reproduced fairly well by the model calculation; in the case of partial cross section, i.e., isomeric cross section, however, the agreement between experiment and theory is only in approximate terms. The same

is true for the isomeric cross-section ratio as well. Despite the similar nuclear structure of the two isomeric pairs, the trends in the isomeric cross-section ratios are not necessarily similar. As regards the effect of the reaction channel, the isomeric cross-section ratio is higher in the (n,p) reaction than in other reactions.

ACKNOWLEDGMENTS

We thank the crew of the compact cyclotron CV28 at Jülich for numerous irradiations. C.D.N. acknowledges the Deutscher Akademischer Austauschdienst (DAAD) for research work at Jülich.

[1] CINDA-A, The Index to Literature and Computer Files on Microscopic Neutron Data (IAEA, Vienna, 1990); CINDA 2000, The Index to Literature and Computer Files on Microscopic Neutron Data (IAEA, Vienna, 2000).
[2] V. McLane, C. L. Dunford, and P. F. Rose, *Neutron Cross Sections* (Academic, New York, 1988), Vol. 2.
[3] E.B. Paul and R.L. Clark, Can. J. Phys. **31**, 267 (1953).
[4] R.E. Wood, W.S. Cook, J.R. Goodgame, and R.W. Fink, Phys. Rev. **154**, 1108 (1967).
[5] G.P. Vinitskaja, V.N. Levkovskii, V.V. Sokolskii, and I.V. Kazachevskii, Sov. J. Nucl. Phys. **5**, 839 (1967).
[6] R. Vänskä and R. Rieppo, Nucl. Instrum. Methods **179**, 525 (1967).
[7] N. Ranakumar, E. Kondaiah, and R.W. Fink, Nucl. Phys. **A122**, 679 (1968).
[8] J. Károlyi, J. Csikai, and G. Petö, Nucl. Phys. **A122**, 234 (1968).
[9] F. Demichelis, M. Guideti, E. Miraldi, and C. Oldano, Nuovo Cimento B **58**, 177 (1968).
[10] S.M. Qaim, Nucl. Phys. **A185**, 614 (1972).
[11] W. Grochulski, S. El-Konsol, and A. Marcinkowski, Acta Phys. Pol. **56**, 139 (1975).
[12] J.L. Casanova and M.L. Sanchez, An. R. Soc. Fis. Esp. Quim. **72**, 186 (1976).
[13] R. Rieppo, J.K. Keinanen, and J. Valkonen J. Inorg. Nucl. Chem. **38**, 1927 (1976).
[14] N.I. Molla and S.M. Qaim, Nucl. Phys. **A283**, 269 (1977).
[15] H.M. Hoang, U. Garuska, D. Kielan, A. Marcinkowski, and B. Zweiglinski, Z. Phys. A **342**, 283 (1992).
[16] C. Konno, Y. Ikeda, K. Oishi, K. Kawade, H. Yamamoto, and H. Maekawa, Japan Atomic Energy Research Institute Report No. 1329, 1993.
[17] D.C. Santry and J.P. Butler, Can. J. Phys. **42**, 2536 (1972).
[18] C. Nesaraja, K.-H. Linse, S. Spellerberg, A. Sudár, A. Suhaimi, and S.M. Qaim, Radiochim. Acta **86**, 1 (1999).
[19] S. M. Qaim, in *Proceedings of the International Conference on Nuclear Data for Science and Technology*, edited by J. K. Dickens (American Nuclear Society Inc., LaGrange Park, 1994), p. 186.
[20] S.M. Qaim, A. Mushtaq, and M. Uhl, Phys. Rev. C **38**, 645 (1988).
[21] S. Sudár and S.M. Qaim, Phys. Rev. C **53**, 2885 (1996).
[22] B. Strohmaier, M. Fassbender, and S.M. Qaim, Phys. Rev. C **56**, 2654 (1997).
[23] F. Cserpák, S. Sudár, J. Csikai, and S.M. Qaim, Phys. Rev. C **49**, 1525 (1994).
[24] I.-G. Birn, B. Strohmaier, H. Freiesleben, and S.M. Qaim, Phys. Rev. C **52**, 2546 (1995).
[25] S.M. Qaim, R. Wólfle, M.M. Rahman, and H. Ollig, Nucl. Sci. Eng. **88**, 143 (1984).
[26] A. Grallert, J. Csikai, S.M. Qaim, and J. Knieper, Nucl. Instrum. Methods Phys. Res. A **334**, 154 (1993).
[27] I.-G. Birn, KFA Report No. INC-IB-1, 1992.
[28] S. Cabral, B. Börker, H. Klein, and W. Mannhart, Nucl. Sci. Eng. **106**, 308 (1990).
[29] N.P. Kocherov and P.K. McLaughlin, *The International Radiation Dosimetry File, version 2* (IAEA, Vienna, 1993).
[30] E. Browne and R. B. Firestone, *Table of Radioactive Isotopes* (Wiley, New York, 1986).
[31] R. B. Firestone, *Table of Isotopes* (Wiley, New York, 1996).
[32] M. Uhl and B. Strohmaier, *Computer Code for Particle Induced Activation Cross Section and Related Quantities* (Institut für Radiumforschung und Kernphysik, Vienna, 1976).
[33] O. Bersillon, *Un programme de modele optique spherique* (Centre d'Etudes de Bruyères-le Châtel, Paris, 1981).
[34] J.C. Ferrer, J.D. Carlson, and J. Rapaport, Nucl. Phys. **A275**, 125 (1977).
[35] F.G. Perey, Phys. Rev. **131**, 745 (1962).
[36] L. McFadden and G.R. Satchler, Nucl. Phys. **84**, 177 (1966).
[37] M.R. Bhat, Nucl. Data Sheets **58**, 1 (1989).
[38] M.R. Bhat, Nucl. Data Sheets **68**, 579 (1993).
[39] W. Dilg, W. Schantl, and H. Vonach, Nucl. Phys. **A217**, 216 (1973).
[40] S. Sudár, F. Szelecsényi, and S.M. Qaim, Phys. Rev. C **48**, 3115 (1993).